

Prospects for searching for sterile neutrinos with gravitational wave and γ -ray burst joint observations

Lu Feng,^{1,2,*} Tao Han,^{2,*} Jing-Fei Zhang,² and Xin Zhang^{2,3,4,†}

¹*College of Physical Science and Technology, Shenyang Normal University, Shenyang 110034, China*

²*Key Laboratory of Cosmology and Astrophysics (Liaoning) & College of Sciences, Northeastern University, Shenyang 110819, China*

³*Key Laboratory of Data Analytics and Optimization for Smart Industry (Ministry of Education), Northeastern University, Shenyang 110819, China*

⁴*National Frontiers Science Center for Industrial Intelligence and Systems Optimization, Northeastern University, Shenyang 110819, China*

Sterile neutrinos can influence the evolution of the universe, and thus cosmological observations can be used to detect them. Future gravitational wave (GW) observations can precisely measure absolute cosmological distances, helping to break parameter degeneracies generated by traditional cosmological observations. This advancement can lead to much tighter constraints on sterile neutrino parameters. This work provides a preliminary forecast for detecting sterile neutrinos using third-generation GW detectors in combination with future short γ -ray burst observations from a THESEUS-like telescope, an approach not previously explored in the literature. Both massless and massive sterile neutrinos are considered within the Λ CDM cosmology. We find that using GW data can greatly enhance the detection capability for massless sterile neutrinos, reaching 3σ level. For massive sterile neutrinos, GW data can also greatly assist in improving the parameter constraints, but it seems that effective detection is still not feasible.

I. INTRODUCTION

On 17 August 2017, the first observation of gravitational waves (GW) from a binary neutron star (BNS) merger [1], together with the first joint observation of GW from a BNS merger and its electromagnetic (EM) counterpart [2, 3], marked the beginning of a new era in multi-messenger astronomy and cosmology. The measurement of the GW signal directly provides information on the absolute luminosity distance to the source, while its redshift can be determined by identifying the EM counterpart of the GW source. This establishes an absolute distance-redshift relation, known as the standard siren method, which is crucial for cosmological studies. To date, only one bright siren, GW170817, has been identified. This is insufficient to probe cosmological parameters using current standard sirens, necessitating the use of next-generation GW detectors.

In the future, third-generation (3G) ground-based GW detectors, such as the Einstein Telescope (ET) [4, 5] in Europe and the Cosmic Explorer (CE) [6, 7] in the United States will become operational, with sensitivities improved one order of magnitude over the current detectors, and much more BNS merger events will be observed at much deeper redshifts. Recently, GW standard sirens have been widely discussed in the literature [8–47]. It has been found that future observations of GW standard sirens from the ET and CE will play a crucial role in the estimation of cosmological parameters [14, 16, 22, 25, 26, 28, 37, 38, 43, 46]. In particular, the GW standard sirens can break the parameter

degeneracies generated by the current EM cosmological observations, thereby improving constraints on neutrino mass, see e.g., Refs. [14, 37].

A recent forecast [46] demonstrated that joint observations of BNS by 3G GW detectors and short γ -ray burst (GRB) observations by missions similar to the THESEUS satellite project can improve the constraints on the total active neutrino mass. Therefore, it is crucial to investigate how the combined GW-GRB observations would affect constraints on the sterile neutrino parameters.

The existence of light sterile neutrinos has been suggested by anomalies in short-baseline (SBL) neutrino experiments [48–57]. To explain the SBL neutrino oscillation data, sterile neutrinos with eV-scale masses are required [58–60]. Cosmological observations play a crucial role in constraining the mass of active neutrinos (see, e.g., Refs. [61–108]). Since sterile neutrinos have implications for the evolution of the universe, cosmology can provide an independent test for their existence. For related works on sterile neutrinos, see, e.g., Refs. [109–134].

Currently, one of the most significant challenges in cosmology is the “Hubble tension” [135], which refers to the discrepancy between early and late universe observations. In the past few years, people often considered models that include light sterile neutrinos to alleviate the Hubble constant crisis. This is because when using the cosmic microwave background data to constrain cosmological parameters, the effective number of neutrino species (N_{eff}) is positively correlated with the Hubble constant; if N_{eff} is larger, the derived Hubble constant will also be larger. See, e.g., Refs. [118, 125–128, 130, 131, 134], for related studies. However, in recent years, the results of cosmological observation fits have shown that the effect of using this method to alleviate the Hubble crisis is no longer significant. Nevertheless, due to the significant

* These authors contributed equally to this paper.

† Corresponding author; zhangxin@mail.neu.edu.cn

correlation between N_{eff} and H_0 , precise measurements of the Hubble constant using gravitational wave standard sirens are very helpful for determining the parameters of sterile neutrinos.

Additionally, the main advantage of the standard siren method for measuring the Hubble constant is that it avoids relying on the cosmic distance ladder. Therefore, in the future, the GW standard sirens could become a promising cosmological probe, playing a crucial role in measuring cosmological parameters, including those related to sterile neutrinos.

In this paper, we present a forecast for the search for sterile neutrinos using joint GW-GRB observations. The primary aim of this work is to investigate the impact of future GW standard siren observations on the constraints of sterile neutrino parameters.

This work is organized as follows. In Sec. II, we introduce the methodology used in this work. In Sec. III, we give the constraint results and make some relevant discussions. The conclusion is given in Sec. IV.

II. METHODOLOGY

A. Gravitational wave simulation

In this subsection, we introduce the method of simulating the joint GW standard sirens and GRB events. We consider the THESEUS-like GRB detector in synergy with the 3G GW observation. We use the simulation method as prescribed in Refs. [43, 46]. Here, we provide only a brief overview.

Based on the star formation rate [136–138], the BNS merger rate with redshift is

$$R_m(z) = \frac{\mathcal{R}_m(z)}{1+z} \frac{dV(z)}{dz}, \quad (1)$$

where $dV(z)/dz$ is the comoving volume element, $\mathcal{R}_m(z)$ is the source-frame BNS merger rate is given by

$$\mathcal{R}_m(z) = \int_{t_{\min}}^{t_{\max}} \mathcal{R}_f[t(z) - t_d] P(t_d) dt_d, \quad (2)$$

where t_d is the delay time between the formation of BNS system and merger, $t_{\min} = 20$ Myr is the minimum delay time, $t_{\max} = t_H$ is the maximum delay time, $t(z)$ is the age of the universe at the time of merger, \mathcal{R}_f is the cosmic star formation rate for which we adopt the Madau-Dickinson model [139], $P(t_d)$ is the time delay distribution of the t_d , and we adopt the exponential time delay model [138], which is given by

$$P(t_d) = \frac{1}{\tau} \exp(-t_d/\tau), \quad (3)$$

with an e-fold time of $\tau = 0.1$ Gyr for $t_d > t_{\min}$.

In our calculations, for BNS mergers, we consider the local comoving merger to be $\mathcal{R}_m(z = 0) =$

920 Gpc⁻³ yr⁻¹, which is the estimated median from the O1 LIGO and the O2 LIGO/Virgo observation run [140] and is also consistent with the O3 observation run [141]. We simulate a catalog of BNS merger for 10 years observation. For each source, the location (θ, ϕ) , the polarization angle ψ , the cosine of the inclination angle ι , and the coalescence phase ψ_c are drawn from uniform distributions. For the mass of neutron star (NS) distribution, we employ a Gaussian mass distribution. This distribution has a mean of $1.33 M_\odot$ for the NS mass and a standard deviation of $0.09 M_\odot$, where M_\odot represents the solar mass.

Under the stationary phase approximation [142], the Fourier transform of the frequency-domain GW waveform for a detector network (with N detectors) is given by [143, 144]

$$\tilde{\mathbf{h}}(f) = e^{-i\Phi} \mathbf{h}(f), \quad (4)$$

with the $\mathbf{h}(f)$ is given by

$$\mathbf{h}(f) = \left[\frac{h_1(f)}{\sqrt{S_{n,1}(f)}}, \frac{h_2(f)}{\sqrt{S_{n,2}(f)}}, \dots, \frac{h_N(f)}{\sqrt{S_{n,N}(f)}} \right]^T, \quad (5)$$

where Φ is the $N \times N$ diagonal matrix with $\Phi_{ij} = 2\pi f \delta_{ij} (\mathbf{n} \cdot \mathbf{r}_k)$, \mathbf{n} is the propagation direction of GW, and \mathbf{r}_k is the location of the k -th detector. Here $S_{n,k}(f)$ is the one-side noise power spectral density of the k -th detector, The Fourier transform of the GW waveform of k -th detector is given by

$$h_k(f) = \mathcal{A}_k f^{-7/6} \exp\{i[2\pi f t_c - \pi/4 - 2\psi_c + 2\Psi(f/2)] - \varphi_{k,(2,0)}\}, \quad (6)$$

where the Fourier amplitude can be written as

$$\mathcal{A}_k = \frac{1}{d_L} \sqrt{(F_{+,k}(1 + \cos^2 \iota))^2 + (2F_{\times,k} \cos \iota)^2} \times \sqrt{5\pi/96} \pi^{-7/6} \mathcal{M}_{\text{chirp}}^{5/6}, \quad (7)$$

here the detailed forms of $\Psi(f/2)$ and $\varphi_{k,(2,0)}$ can be found in Refs. [143, 145], d_L is the luminosity distance of the GW source, $\mathcal{M}_{\text{chirp}} = (1+z)\eta^{3/5}M$ is the observed chirp mass, $\eta = m_1 m_2 / M^2$ is the symmetric mass ratio, and $M = m_1 + m_2$ is the total mass of binary system with component masses m_1 and m_2 , $F_{+,k}$ and $F_{\times,k}$ are the antenna response functions of the k -th GW detector, we adopt the GW waveform in the frequency domain, in which the time t is replaced by $t_f = t_c - (5/256)\mathcal{M}_{\text{chirp}}^{-5/3}(\pi f)^{-8/3}$ [143, 145], where t_c is the coalescence time.

In this work, we consider the waveform in the inspiralling stage for the non-spinning BNS system. Here we adopt the restricted Post-Newtonian approximation and calculate the waveform to the 3.5 PN order [145, 146].

After simulating the GW catalog, we need to calculate the signal-to-noise ratio (SNR) for each GW event. The SNR for the detection network of N independent interferometers can be calculated by

$$\rho = (\tilde{\mathbf{h}}|\tilde{\mathbf{h}})^{1/2}. \quad (8)$$

The inner product is defined as

$$(\mathbf{a}|\mathbf{b}) = 2 \int_{f_{\text{lower}}}^{f_{\text{upper}}} \{\mathbf{a}(f)\mathbf{b}^*(f) + \mathbf{a}^*(f)\mathbf{b}(f)\}df, \quad (9)$$

where $*$ represents conjugate transpose, \mathbf{a} and \mathbf{b} are column matrices of the same dimension, the lower cutoff frequency is set to $f_{\text{lower}} = 1$ Hz for ET and $f_{\text{lower}} = 5$ Hz for CE, and $f_{\text{upper}} = 2/(6^{3/2}2\pi M_{\text{obs}})$ is the frequency at the last stable orbit with $M_{\text{obs}} = (m_1 + m_2)(1 + z)$. In this work, we adopt the SNR threshold to be 12 in our simulation.

For the short GRB model, we adopt the model of Gaussian structured jet profile based on the GW170817/GRB170817A [147] observation,

$$L_{\text{iso}}(\theta_v) = L_{\text{on}} \exp\left(-\frac{\theta_v^2}{2\theta_c^2}\right), \quad (10)$$

where θ_v is the viewing angle, $L_{\text{iso}}(\theta_v)$ is the isotropically equivalent luminosity of short GRB observed at different θ_v , $L_{\text{on}} = L_{\text{iso}}(0)$ is the on-axis isotropic luminosity, $\theta_c = 4.7^\circ$ is the characteristic angle of the core, and the direction of the jet is assumed to align with the binary orbital angular momentum, namely $\iota = \theta_v$.

For the distribution of the short GRB, we assume the empirical broken-power-law luminosity function

$$\Phi(L) \propto \begin{cases} (L/L_*)^\alpha, & L < L_*, \\ (L/L_*)^\beta, & L \geq L_*, \end{cases} \quad (11)$$

where L is the isotropic rest frame luminosity in the 1–10000 keV energy range, L_* is the characteristic luminosity that separates the low and high end of the luminosity function, and the slopes describing these regimes are given by α and β , respectively. Following Ref. [148], we adopt $L_* = 2 \times 10^{52}$ erg sec $^{-1}$, $\alpha = -1.95$, and $\beta = -3$. We assume a standard low end cutoff in luminosity of $L_{\text{min}} = 10^{49}$ erg sec $^{-1}$, and we also term the on-axis isotropic luminosity L_{on} as the peak luminosity L . For the THESEUS mission [149], a GRB detection is recorded if the value of observed flux is greater than the flux threshold $P_T = 0.2$ ph s $^{-1}$ cm $^{-2}$ is the 50-300 keV band. For the GRB detection, we assume a duty cycle of 80% and a sky coverage fraction of 0.5. From the GW catalogue which has passed the threshold 12, we can select the GW-GRB events according to the probability distribution $\Phi(L)dL$.

For a network with N independent interferometers, the Fisher information matrix is given by

$$F_{ij} = \left(\frac{\partial \tilde{\mathbf{h}}}{\partial \theta_i} \middle| \frac{\partial \tilde{\mathbf{h}}}{\partial \theta_j} \right) \quad (12)$$

where θ_i denotes nine GW parameters (d_L , $\mathcal{M}_{\text{chirp}}$, η , θ , ϕ , ι , t_c , ψ_c , ψ) for a GW event.

For the total uncertainty of the luminosity distance d_L , we first consider the instrumental error $\sigma_{d_L}^{\text{inst}}$. The

covariance matrix is equal to the inverse of the Fisher information matrix, thus the instrumental error of GW parameter θ_i is

$$\Delta\theta_i = \sqrt{(F^{-1})_{ii}} \quad (13)$$

where F_{ij} is the total Fisher information matrix for the network of N interferometers.

In addition, the weak-lensing error $\sigma_{d_L}^{\text{lens}}$ and the peculiar velocity error $\sigma_{d_L}^{\text{pv}}$ are also considered. The error caused by weak lensing is adopted from Refs. [150, 151],

$$\sigma_{d_L}^{\text{lens}}(z) = \left[1 - \frac{0.3}{\pi/2} \arctan(z/0.073) \right] \times d_L(z) \times 0.066 \left[\frac{1 - (1+z)^{-0.25}}{0.25} \right]^{1.8}. \quad (14)$$

For the error caused by the peculiar velocity of the GW source is given by [152]

$$\sigma_{d_L}^{\text{pv}}(z) = d_L(z) \times \left[1 + \frac{c(1+z)^2}{H(z)d_L(z)} \right] \frac{\sqrt{\langle v^2 \rangle}}{c}, \quad (15)$$

where c is the speed of light in vacuum, $H(z)$ is the Hubble parameter, and $\sqrt{\langle v^2 \rangle}$ is the peculiar velocity of the GW source with respect to the Hubble flow is roughly set to $\sqrt{\langle v^2 \rangle} = 500$ km s $^{-1}$.

Hence, the total error of d_L can be written as

$$\sigma_{d_L} = \sqrt{(\sigma_{d_L}^{\text{inst}})^2 + (\sigma_{d_L}^{\text{lens}})^2 + (\sigma_{d_L}^{\text{pv}})^2}. \quad (16)$$

B. Other cosmological observations

For comparison, we also employ three current EM cosmological observations, i.e., the cosmic microwave background (CMB) data, the baryon acoustic oscillation (BAO) data, and the type Ia supernova (SN) data. The details of these data are listed as follows.

The CMB data: the CMB likelihood including the TT, TE, EE spectra at $l \geq 30$, the low- l temperature commander likelihood, and the low- l SimAll EE likelihood, from the Planck 2018 data release [153].

The BAO data: the measurements from 6dFGs at $z_{\text{eff}} = 0.106$ [154], the SDSS-MGS at $z_{\text{eff}} = 0.15$ [155], and BOSS-DR12 at $z_{\text{eff}} = 0.38$, $z_{\text{eff}} = 0.51$, and $z_{\text{eff}} = 0.61$ [156].

The SN data: the Pantheon sample comprised of 1048 data points from the Pantheon compilation [157].

C. Methods of constraining cosmological parameters

In this paper, we will consider both cases of massless and massive sterile neutrinos in the framework of standard model (Λ CDM) of cosmology. For the Λ CDM

model, the base parameter set (including six free parameters) is

$$\mathbf{P} = \{\omega_b, \omega_c, 100\theta_{\text{MC}}, \tau, \ln(10^{10}A_s), n_s\},$$

where $\omega_b \equiv \Omega_b h^2$ and $\omega_c \equiv \Omega_c h^2$ are the physical densities of baryon and cold dark matter, respectively, θ_{MC} is the ratio (multiplied by 100) between the sound horizon and the angular diameter distance at the time of last-scattering, τ is the optical depth to the reionization, A_s is the amplitude of the primordial curvature perturbation, and n_s is the scalar spectral index.

When we consider massless sterile neutrinos (as the dark radiation) in the Λ CDM model, an additional parameter N_{eff} (the effective number of relativistic species) need to be added in the model, and this case is called Λ CDM+ N_{eff} model in this paper. When the massive sterile neutrinos are considered in the Λ CDM model, two extra free parameters, the N_{eff} and $m_{\nu, \text{sterile}}^{\text{eff}}$ (the effective sterile neutrino mass) need to be added in the model, and this case is called Λ CDM+ N_{eff} + $m_{\nu, \text{sterile}}^{\text{eff}}$ model in this paper. Thus, the Λ CDM+ N_{eff} model has seven independent parameters, and the Λ CDM+ N_{eff} + $m_{\nu, \text{sterile}}^{\text{eff}}$ model has eight independent parameters. Note that in both the massless and massive sterile neutrino cases the total mass of active neutrinos is fixed at $\sum m_\nu = 0.06$ eV.

For the GW standard siren observation with N data point, the χ^2 function is defined as

$$\chi_{\text{GW}}^2 = \sum_{i=1}^N \left[\frac{d_L^i - d_L(z_i; \vec{\Omega})}{\sigma_{d_L}^i} \right]^2, \quad (17)$$

where z_i , d_L^i , and $\sigma_{d_L}^i$ are the i -th GW redshift, luminosity distance, and the measurement error of the luminosity distance, respectively, $\vec{\Omega}$ denotes the set of cosmological parameters.

In this work, we present the first forecast for the search for sterile neutrinos using joint GW-GRB observation. We use the public Markov-chain Monte Carlo (MCMC) package CosmoMC [158] to constrain sterile neutrino and other cosmological parameters. To demonstrate the impact of simulated GW data on constraining sterile neutrino parameters, we will consider all the different cases of 3G GW observations, the single ET, the single CE, the CE-CE network (one CE in the United States with 40-km arm length and another one in Australia with 20-km arm length, abbreviated as 2CE hereafter), and the ET-CE-CE network (one ET detector and two CE-like detectors, abbreviated as ET2CE hereafter) to analysis. We utilize the sensitivity curves of ET from Ref. [159] and for CE from Ref. [160], as shown in Fig. 1. For the GW detector, in view of the high uncertainty of the duty cycle, we only calculate the ideal scenario assuming a 100% duty cycle for all detectors, as discussed in Ref. [161]. The specific parameters characterizing the geometry of GW detector (latitude φ , longitude λ , opening angle ζ , and arm bisector angle γ) are detailed in Table I. The number of GW standard sirens in the subsequent cosmological analysis

are shown in Table II and their redshift distributions are shown in Fig. 2.

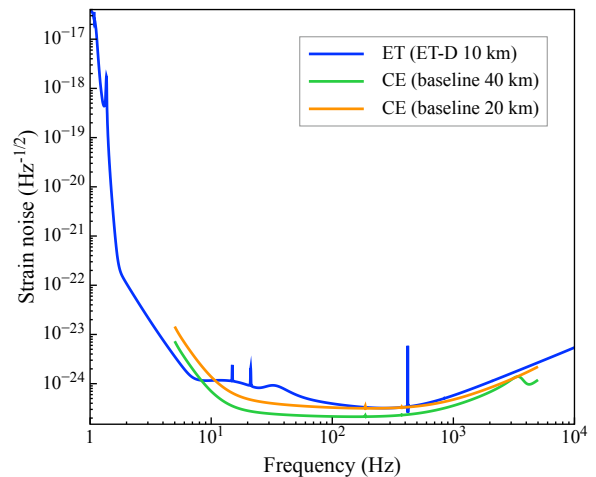


FIG. 1. Sensitivity curves of the 3G GW detectors considered in this work.

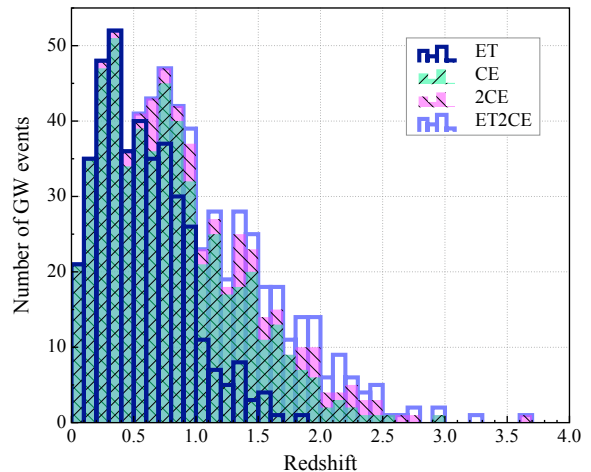


FIG. 2. Redshift distributions of BNS detected by THESEUS in synergy with ET, CE, 2CE, and ET2CE for a 10-year observation.

To enable a clear comparison of constraints within the same parameter space, we use the best-fit values of cosmological parameters from the CMB+BAO+SN data combination as the fiducial values to simulate the GW data for each cosmological model. For simplicity, we use “CBS” to denote the joint CMB+BAO+SN data combination. Thus, in our analysis, we use five data combinations: (1) CBS, (2) CBS+ET, (3) CBS+CE, (4) CBS+2CE, and (5) CBS+ET2CE. We will report the constraint results in the next section.

TABLE I. The specific coordinate parameters considered in this work.

GW detector	φ (deg)	λ (deg)	γ (deg)	ζ (deg)
Einstein Telescope, Europe	40.443	9.457	0.000	60
Cosmic Explorer, USA	43.827	-112.825	45.000	90
Cosmic Explorer, Australia	-34.000	145.000	90.000	90

TABLE II. Numbers of GW standard sirens in cosmological analysis, triggered by THESEUS in synergy with ET, CE, 2CE, and ET2CE, respectively.

Detection strategy	ET	CE	2CE	ET2CE
Number of GW standard sirens	400	538	600	640

III. RESULTS AND DISCUSSION

In this section, we report the constraint results for the Λ CDM+ N_{eff} and Λ CDM+ $N_{\text{eff}}+m_{\nu, \text{sterile}}^{\text{eff}}$ models using the CBS, CBS+ET, CBS+CE, CBS+2CE, and CBS+ET2CE data combinations and analyze how the GW standard sirens affects the cosmological constraints on the sterile neutrino parameters. The fitting results are shown in Figs. 3 and 4 and Tables III and IV. In the tables, we quote $\pm 1\sigma$ errors for the parameters, but for the parameters that cannot be well constrained, e.g., the sterile neutrino parameters N_{eff} and $m_{\nu, \text{sterile}}^{\text{eff}}$, we quote the 2σ upper limits. For a parameter ξ , we use $\sigma(\xi)$ and $\varepsilon(\xi) = \sigma(\xi)/\xi$ represent its absolute error and relative error, respectively.

A. The case of massless sterile neutrino

The massless sterile neutrinos serve as the dark radiation, and thus in this case N_{eff} is treated as a free parameter, the total relativistic energy density of radiation is given by

$$\rho_r = [1 + N_{\text{eff}} \frac{7}{8} (\frac{4}{11})^{\frac{4}{3}}] \rho_\gamma,$$

where ρ_γ is the photon energy density. In the Λ CDM model, $N_{\text{eff}} = 3.046$, and so $\Delta N_{\text{eff}} = N_{\text{eff}} - 3.046 > 0$ indicates the presence of extra relativistic particle species in the early universe, and in this paper we take the fit results of $\Delta N_{\text{eff}} > 0$ as evidence of the existence of massless sterile neutrinos.

In Table III, we find that the CBS data provides only an upper limit, $N_{\text{eff}} < 3.464$, indicating that the existence of massless sterile neutrinos is not favored by the CBS data. However, when GW standard sirens are included in the data combination, the results change significantly. After considering the GW data, we obtain $N_{\text{eff}} = 3.209 \pm 0.060$ for CBS+ET, $N_{\text{eff}} = 3.209 \pm 0.056$ for CBS+CE, $N_{\text{eff}} = 3.210_{-0.056}^{+0.055}$ for CBS+2CE, and $N_{\text{eff}} = 3.208_{-0.055}^{+0.054}$ for CBS+ET2CE, which indicates a

detection of $\Delta N_{\text{eff}} > 0$ at the 2.717σ , 2.911σ , 2.929σ , and 2.945σ significance levels, respectively. Obviously, the GW data can indeed effectively improve the constraints on the massless sterile neutrino parameter N_{eff} (see also Fig. 3). Due to the ability of GW observations to precisely measure the Hubble constant, this leads to a strong breaking of the degeneracy between N_{eff} and H_0 , thus allowing for a precise determination of N_{eff} in joint constraints. We find that, under these circumstances, GW observations can significantly enhance the detection of massless sterile neutrinos (dark radiation), reaching about 3σ level.

In the right panel of Fig. 3, we show the two-dimensional posterior distribution contours (1σ and 2σ) in the $N_{\text{eff}}-H_0$ and $N_{\text{eff}}-\Omega_m$ planes for the Λ CDM+ N_{eff} model using CBS, CBS+ET, CBS+CE, CBS+2CE, and CBS+ET2CE data combinations. We can see that N_{eff} is in positive correlation with H_0 by using the CBS data combination. However, after adding the GW data, this correlation becomes negligible, indicating that the degeneracy between N_{eff} and H_0 is effectively broken by the GW observations. In addition, we can also clearly see that when considering the GW data, the parameter space is greatly shrunk in each planes and the constraints on cosmological parameters of H_0 and Ω_m become much tighter.

In Table III, we also show absolute and relative errors of H_0 and Ω_m from the CBS, CBS+ET, CBS+CE, CBS+2CE, and CBS+ET2CE data combinations. Compared to the CBS data, we find that the accuracy of the H_0 constraint improves by 93.253% for CBS+ET, 93.193% for CBS+CE, 93.614% for CBS+2CE, and 93.855% for CBS+ET2CE, respectively. Similarly, the accuracy of the Ω_m constraint improves by 37.190% for CBS+ET, 41.322% for CBS+CE, 42.149% for CBS+2CE, and 42.975% for CBS+ET2CE, respectively. Obviously, the GW data can indeed effectively improve the constraints on the parameters H_0 and Ω_m .

TABLE III. Fitting results of the Λ CDM+ N_{eff} model by using the CBS, CBS+ET, CBS+CE, CBS+2CE, and CBS+ET2CE data combinations. We quote $\pm 1\sigma$ errors for the parameters, but for the parameters that cannot be well constrained, we quote the 2σ upper limits. Here, H_0 is in units of $\text{km s}^{-1} \text{Mpc}^{-1}$.

Model	CBS	CBS+ET	CBS+CE	CBS+2CE	CBS+ET2CE
$\Omega_b h^2$	0.02247 ± 0.00015	0.02248 ± 0.00011	0.02248 ± 0.00011	0.02248 ± 0.00011	0.02248 ± 0.00011
$\Omega_c h^2$	$0.1220^{+0.0017}_{-0.0028}$	0.1217 ± 0.0017	0.1217 ± 0.0016	0.1217 ± 0.0016	0.1217 ± 0.0016
$100\theta_{MC}$	$1.04046^{+0.00043}_{-0.00037}$	1.04050 ± 0.00036	$1.04050^{+0.00034}_{-0.00035}$	1.04049 ± 0.00035	1.04050 ± 0.00034
τ	$0.0558^{+0.0074}_{-0.0083}$	$0.0558^{+0.0075}_{-0.0082}$	$0.0559^{+0.0074}_{-0.0082}$	$0.0559^{+0.0075}_{-0.0082}$	$0.0558^{+0.0072}_{-0.0082}$
n_s	$0.9697^{+0.0046}_{-0.0057}$	0.9696 ± 0.0030	$0.9696^{+0.0030}_{-0.0031}$	0.9697 ± 0.0030	0.9697 ± 0.0029
$\ln(10^{10} A_s)$	$3.051^{+0.016}_{-0.018}$	3.050 ± 0.016	3.050 ± 0.016	3.050 ± 0.016	3.050 ± 0.016
σ_8	$0.8177^{+0.0083}_{-0.0101}$	$0.817^{+0.0082}_{-0.0081}$	0.8169 ± 0.0078	0.8171 ± 0.0079	0.8169 ± 0.0077
Ω_m	$0.3077^{+0.0060}_{-0.0061}$	0.3071 ± 0.0038	$0.3071^{+0.0035}_{-0.0036}$	0.3071 ± 0.0035	$0.3070^{+0.0034}_{-0.0035}$
H_0	$68.670^{+0.640}_{-1.020}$	$68.671^{+0.057}_{-0.055}$	$68.671^{+0.056}_{-0.057}$	$68.671^{+0.052}_{-0.054}$	$68.672^{+0.052}_{-0.050}$
N_{eff}	< 3.464	3.209 ± 0.060	3.209 ± 0.056	$3.210^{+0.055}_{-0.056}$	$3.208^{+0.054}_{-0.055}$
$\Delta N_{\text{eff}} > 0$...	2.717σ	2.911σ	2.929σ	2.945σ
$\sigma(\Omega_m)$	0.00605	0.00380	0.00355	0.00350	0.00345
$\sigma(H_0)$	0.8300	0.0560	0.0565	0.0530	0.0510
$\varepsilon(\Omega_m)$	1.966%	1.237%	1.156%	1.140%	1.124%
$\varepsilon(H_0)$	1.209%	0.082%	0.082%	0.077%	0.074%

TABLE IV. Fitting results of the Λ CDM+ $N_{\text{eff}}+m_{\nu, \text{sterile}}^{\text{eff}}$ model by using the CBS, CBS+ET, CBS+CE, CBS+2CE, and CBS+ET2CE data combinations. We quote $\pm 1\sigma$ errors for the parameters, but for the parameters that cannot be well constrained, we quote the 2σ upper limits. Here, H_0 is in units of $\text{km s}^{-1} \text{Mpc}^{-1}$ and $m_{\nu, \text{sterile}}^{\text{eff}}$ is in units of eV.

Model	CBS	CBS+ET	CBS+CE	CBS+2CE	CBS+ET2CE
$\Omega_b h^2$	$0.02247^{+0.00015}_{-0.00016}$	0.02249 ± 0.00012	0.02249 ± 0.00012	0.02249 ± 0.00012	0.02249 ± 0.00012
$\Omega_c h^2$	$0.1198^{+0.0036}_{-0.0031}$	$0.1193^{+0.0033}_{-0.0018}$	$0.1193^{+0.0032}_{-0.0017}$	$0.1195^{+0.0031}_{-0.0017}$	$0.1194^{+0.0030}_{-0.0017}$
$100\theta_{MC}$	$1.04059^{+0.00047}_{-0.00033}$	$1.04071^{+0.00041}_{-0.00035}$	$1.04071^{+0.00040}_{-0.00035}$	$1.04070^{+0.00040}_{-0.00036}$	$1.04071^{+0.00039}_{-0.00036}$
τ	$0.0561^{+0.0073}_{-0.0083}$	$0.0566^{+0.0074}_{-0.0082}$	$0.0566^{+0.0074}_{-0.0082}$	$0.0568^{+0.0074}_{-0.0083}$	$0.0569^{+0.0074}_{-0.0083}$
n_s	$0.9681^{+0.0047}_{-0.0065}$	0.9684 ± 0.0033	0.9684 ± 0.0033	0.9684 ± 0.0033	$0.9684^{+0.0033}_{-0.0032}$
$\ln(10^{10} A_s)$	$3.048^{+0.016}_{-0.018}$	$3.048^{+0.016}_{-0.017}$	$3.048^{+0.016}_{-0.017}$	3.048 ± 0.016	3.048 ± 0.016
σ_8	$0.796^{+0.024}_{-0.014}$	$0.795^{+0.022}_{-0.012}$	$0.795^{+0.022}_{-0.012}$	$0.796^{+0.021}_{-0.012}$	$0.796^{+0.022}_{-0.012}$
Ω_m	0.3114 ± 0.0064	$0.3096^{+0.0032}_{-0.0052}$	$0.3096^{+0.0032}_{-0.0050}$	$0.3097^{+0.0033}_{-0.0049}$	$0.3096^{+0.0033}_{-0.0048}$
H_0	$68.150^{+0.500}_{-1.000}$	$68.156^{+0.055}_{-0.053}$	$68.156^{+0.054}_{-0.053}$	$68.156^{+0.054}_{-0.053}$	$68.156^{+0.054}_{-0.050}$
N_{eff}	< 3.446	$3.148^{+0.039}_{-0.094}$	$3.148^{+0.040}_{-0.090}$	$3.150^{+0.043}_{-0.089}$	$3.150^{+0.042}_{-0.089}$
$m_{\nu, \text{sterile}}^{\text{eff}}$	< 0.5789	< 0.4842	< 0.4772	< 0.4321	< 0.4226
$\Delta N_{\text{eff}} > 0$...	1.085σ	1.133σ	1.169σ	1.169σ
$\sigma(\Omega_m)$	0.00640	0.00420	0.00410	0.00410	0.00405
$\sigma(H_0)$	0.7500	0.0540	0.0535	0.0535	0.0520
$\varepsilon(\Omega_m)$	2.055%	1.357%	1.324%	1.324%	1.308%
$\varepsilon(H_0)$	1.101%	0.079%	0.078%	0.078%	0.076%

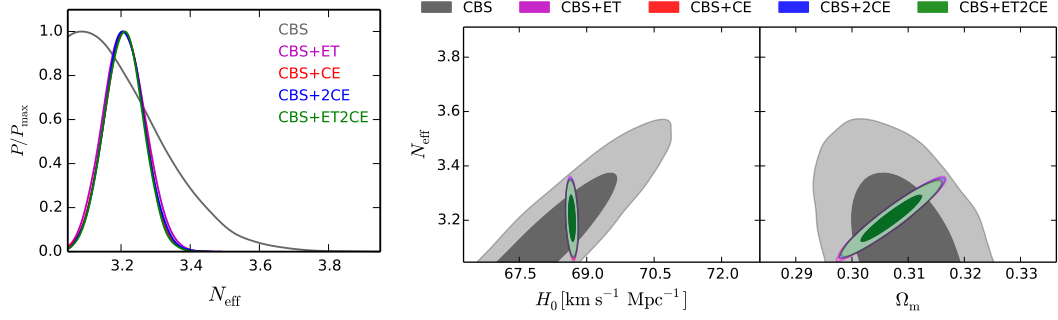


FIG. 3. Constraint results for the $\Lambda\text{CDM}+N_{\text{eff}}$ model from the CBS, CBS+ET, CBS+CE, CBS+2CE, and CBS+ET2CE data combinations. One-dimensional marginalized posterior distribution for N_{eff} (left panel), and two-dimensional marginalized posterior contours (1σ and 2σ) in the H_0-N_{eff} and Ω_m-N_{eff} planes (right panel).

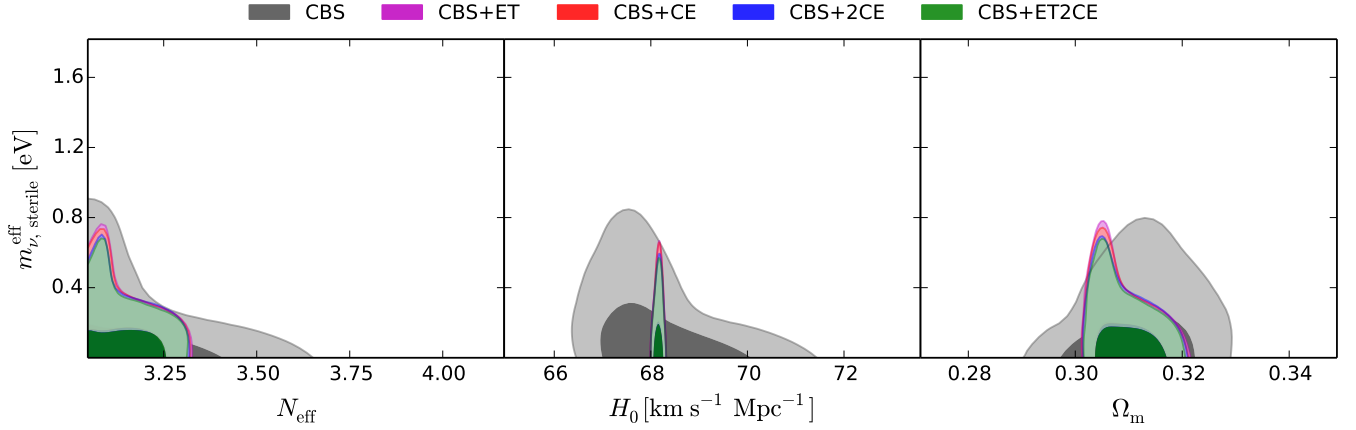


FIG. 4. Two-dimensional marginalized posterior contours (1σ and 2σ) in the $N_{\text{eff}}-m_{\nu,\text{sterile}}^{\text{eff}}$, $H_0-m_{\nu,\text{sterile}}^{\text{eff}}$, $\Omega_m-m_{\nu,\text{sterile}}^{\text{eff}}$ planes for the $\Lambda\text{CDM}+N_{\text{eff}}+m_{\nu,\text{sterile}}^{\text{eff}}$ model from the constraints of the CBS, CBS+ET, CBS+CE, CBS+2CE, and CBS+ET2CE data combinations.

B. The case of massive sterile neutrino

In this subsection, we investigated how GW standard sirens on constraint the massive sterile neutrino parameters. Hence, the requirement of $N_{\text{eff}} > 3.046$ still holds.

From Table IV, we obtain $N_{\text{eff}} < 3.446$ by using CBS data. After adding the GW data, the constraint results become $N_{\text{eff}} = 3.148^{+0.039}_{-0.094}$ for CBS+ET, $N_{\text{eff}} = 3.148^{+0.039}_{-0.090}$ for CBS+CE, $N_{\text{eff}} = 3.150^{+0.043}_{-0.089}$ for CBS+2CE, and $N_{\text{eff}} = 3.150^{+0.042}_{-0.089}$ for CBS+ET2CE, respectively. We find that N_{eff} cannot be well constrained using the CBS data, but the addition of GW data can significantly improve the constraint on N_{eff} , favoring $\Delta N_{\text{eff}} > 0$ at 1.085σ (CBS+ET), 1.133σ (CBS+CE), 1.169σ (CBS+2CE), and 1.169σ (CBS+ET2CE) statistical significance, respectively. For the mass of sterile neutrino, the CBS data give $m_{\nu,\text{sterile}}^{\text{eff}} < 0.5789$ eV and further including the GW data leads to results of $m_{\nu,\text{sterile}}^{\text{eff}} < 0.4842$ eV (CBS+ET), $m_{\nu,\text{sterile}}^{\text{eff}} < 0.4772$ eV (CBS+CE), $m_{\nu,\text{sterile}}^{\text{eff}} < 0.4321$ eV (CBS+2CE), and $m_{\nu,\text{sterile}}^{\text{eff}} < 0.4226$ eV (CBS+ET2CE), respectively. Ev-

idently, adding GW data tightens the constraint on $m_{\nu,\text{sterile}}^{\text{eff}}$ significantly, which is in accordance with the conclusions in previous studies active neutrinos mass by using the GW data [14, 37, 46]. Therefore, the GW data also play an important role in constraining the mass of sterile neutrinos.

In Fig. 4, we show two-dimensional marginalized posterior contours (1σ and 2σ) in the $N_{\text{eff}}-m_{\nu,\text{sterile}}^{\text{eff}}$, $H_0-m_{\nu,\text{sterile}}^{\text{eff}}$, $\Omega_m-m_{\nu,\text{sterile}}^{\text{eff}}$ planes for the $\Lambda\text{CDM}+N_{\text{eff}}+m_{\nu,\text{sterile}}^{\text{eff}}$ model. We can clearly see that when further considering the GW data, the parameter space is also greatly shrunk and the constraints on H_0 and Ω_m also become much tighter. From Table IV, we find that the constraints on H_0 and Ω_m could be improved by 92.800% and 34.375%, respectively, when adding the ET data to the CBS data, 92.867% and 35.938% for the case of CE, 92.867% and 35.938% for the case of 2CE, and 93.067% and 36.719% for the case of ET2CE, respectively. These result in accordance with the conclusions for both the case of massless sterile neutrinos in this study and active neutrinos mass in previous studies [14, 37, 46]. Therefore, the inclusion of GW data

can significantly improve constraints on most cosmological parameters, particularly H_0 and Ω_m .

IV. CONCLUSION

This work aims to forecast the search for sterile neutrinos using joint GW-GRB observations. We consider two cases of massless and massive sterile neutrinos, corresponding to the Λ CDM+ N_{eff} and Λ CDM+ $N_{\text{eff}}+m_{\nu,\text{sterile}}^{\text{eff}}$ models, respectively. We consider four GW detection observation strategies, i.e., ET, CE, the 2CE network, and the ET2CE network, to perform cosmological analysis. To evaluate the impact of GW data on the constraints of sterile neutrino parameters, we also considered existing CMB+BAO+SN data for comparison and combination.

For the Λ CDM+ N_{eff} model, in the case of using CMB+BAO+SN, only upper limits on N_{eff} can be obtained. Further adding the GW data tightens the N_{eff} significantly, and in this case the preference of $\Delta N_{\text{eff}} > 0$ at about 3σ level. Therefore, GW standard siren observations can greatly assist in the detection of massless sterile neutrinos.

For the Λ CDM+ $N_{\text{eff}}+m_{\nu,\text{sterile}}^{\text{eff}}$ model, only upper limits on N_{eff} and $m_{\nu,\text{sterile}}^{\text{eff}}$ can be derived by using the CMB+BAO+SN data. Further including GW data significantly improves the constraints, and we find that the GW data give a rather tight upper limit on $m_{\nu,\text{sterile}}^{\text{eff}}$ and favor $\Delta N_{\text{eff}} > 0$ at about 1.1σ level. This results also seems to favor a massless sterile neutrinos.

Furthermore, we find that the GW data can significantly enhances the accuracy of constraints on the derived parameters H_0 and Ω_m . The accuracy of H_0 improves by approximately 93% and the accuracy of Ω_m increases by about 37% to 42%, when the GW data are included in the cosmological fit.

ACKNOWLEDGMENTS

This work was supported by the National Natural Science Foundation of China (Grant Nos. 12305069, 11947022, 12473001, 11975072, 11875102, and 11835009), the National SKA Program of China (Grants Nos. 2022SKA0110200 and 2022SKA0110203), the Program of the Education Department of Liaoning Province (Grant No. JYTMS20231695), and the National 111 Project (Grant No. B16009).

-
- [1] B. P. Abbott *et al.* (LIGO Scientific, Virgo), *Phys. Rev. Lett.* **119**, 161101 (2017), [arXiv:1710.05832 \[gr-qc\]](#).
 - [2] B. P. Abbott *et al.* (LIGO Scientific, Virgo, Fermi GBM, INTEGRAL, IceCube, AstroSat Cadmium Zinc Telluride Imager Team, IPN, Insight-Hxmt, ANTARES, Swift, AGILE Team, 1M2H Team, Dark Energy Camera GW-EM, DES, DLT40, GRAWITA, Fermi-LAT, ATCA, ASKAP, Las Cumbres Observatory Group, OzGrav, DWF (Deeper Wider Faster Program), AST3, CAASTRO, VINROUGE, MASTER, J-GEM, GROWTH, JAGWAR, CaltechNRAO, TTU-NRAO, NuSTAR, Pan-STARRS, MAXI Team, TZAC Consortium, KU, Nordic Optical Telescope, ePESSTO, GROND, Texas Tech University, SALT Group, TOROS, BOOTES, MWA, CALET, IKI-GW Follow-up, H.E.S.S., LOFAR, LWA, HAWC, Pierre Auger, ALMA, Euro VLBI Team, Pi of Sky, Chandra Team at McGill University, DFN, ATLAS Telescopes, High Time Resolution Universe Survey, RIMAS, RATIR, SKA South Africa/MeerKAT), *Astrophys. J. Lett.* **848**, L12 (2017), [arXiv:1710.05833 \[astro-ph.HE\]](#).
 - [3] M. C. Díaz *et al.* (TOROS), *Astrophys. J. Lett.* **848**, L29 (2017), [arXiv:1710.05844 \[astro-ph.HE\]](#).
 - [4] “ET,” <https://www.et-gw.eu/>.
 - [5] M. Punturo *et al.*, *Class. Quant. Grav.* **27**, 194002 (2010).
 - [6] “CE,” <https://cosmicexplorer.org/>.
 - [7] B. P. Abbott *et al.* (LIGO Scientific), *Class. Quant. Grav.* **34**, 044001 (2017), [arXiv:1607.08697 \[astro-ph.IM\]](#).
 - [8] R.-G. Cai and T. Yang, *Phys. Rev. D* **95**, 044024 (2017), [arXiv:1608.08008 \[astro-ph.CO\]](#).
 - [9] R.-G. Cai and T. Yang, *EPJ Web Conf.* **168**, 01008 (2018), [arXiv:1709.00837 \[astro-ph.CO\]](#).
 - [10] T. Liu, X. Zhang, and W. Zhao, *Phys. Lett. B* **777**, 286 (2018), [arXiv:1711.08991 \[astro-ph.CO\]](#).
 - [11] R.-G. Cai, T.-B. Liu, X.-W. Liu, S.-J. Wang, and T. Yang, *Phys. Rev. D* **97**, 103005 (2018), [arXiv:1712.00952 \[astro-ph.CO\]](#).
 - [12] E. Berti, K. Yagi, and N. Yunes, *Gen. Rel. Grav.* **50**, 46 (2018), [arXiv:1801.03208 \[gr-qc\]](#).
 - [13] Y.-F. Cai, C. Li, E. N. Saridakis, and L. Xue, *Phys. Rev. D* **97**, 103513 (2018), [arXiv:1801.05827 \[gr-qc\]](#).
 - [14] L.-F. Wang, X.-N. Zhang, J.-F. Zhang, and X. Zhang, *Phys. Lett. B* **782**, 87 (2018), [arXiv:1802.04720 \[astro-ph.CO\]](#).
 - [15] W. Zhao, B. S. Wright, and B. Li, *JCAP* **10**, 052 (2018), [arXiv:1804.03066 \[astro-ph.CO\]](#).
 - [16] X.-N. Zhang, L.-F. Wang, J.-F. Zhang, and X. Zhang, *Phys. Rev. D* **99**, 063510 (2019), [arXiv:1804.08379 \[astro-ph.CO\]](#).
 - [17] M. Du, W. Yang, L. Xu, S. Pan, and D. F. Mota, *Phys. Rev. D* **100**, 043535 (2019), [arXiv:1812.01440 \[astro-ph.CO\]](#).
 - [18] J.-h. He, *Phys. Rev. D* **100**, 023527 (2019), [arXiv:1903.11254 \[astro-ph.CO\]](#).
 - [19] W. Yang, S. Pan, E. Di Valentino, B. Wang, and A. Wang, *JCAP* **05**, 050 (2020), [arXiv:1904.11980 \[astro-ph.CO\]](#).
 - [20] W. Yang, S. Vagnozzi, E. Di Valentino, R. C. Nunes, S. Pan, and D. F. Mota, *JCAP* **07**, 037 (2019), [arXiv:1905.08286 \[astro-ph.CO\]](#).
 - [21] X. Zhang, *Sci. China Phys. Mech. Astron.* **62**, 110431 (2019), [arXiv:1905.11122 \[astro-ph.CO\]](#).

- [22] J.-F. Zhang, H.-Y. Dong, J.-Z. Qi, and X. Zhang, *Eur. Phys. J. C* **80**, 217 (2020), arXiv:1906.07504 [astro-ph.CO].
- [23] R. R. A. Bacheaga, A. A. Costa, E. Abdalla, and K. S. F. Fornazier, *JCAP* **05**, 021 (2020), arXiv:1906.08909 [astro-ph.CO].
- [24] L.-F. Wang, Z.-W. Zhao, J.-F. Zhang, and X. Zhang, *JCAP* **11**, 012 (2020), arXiv:1907.01838 [astro-ph.CO].
- [25] J.-F. Zhang, M. Zhang, S.-J. Jin, J.-Z. Qi, and X. Zhang, *JCAP* **09**, 068 (2019), arXiv:1907.03238 [astro-ph.CO].
- [26] H.-L. Li, D.-Z. He, J.-F. Zhang, and X. Zhang, *JCAP* **06**, 038 (2020), arXiv:1908.03098 [astro-ph.CO].
- [27] Z.-W. Zhao, L.-F. Wang, J.-F. Zhang, and X. Zhang, *Sci. Bull.* **65**, 1340 (2020), arXiv:1912.11629 [astro-ph.CO].
- [28] S.-J. Jin, D.-Z. He, Y. Xu, J.-F. Zhang, and X. Zhang, *JCAP* **03**, 051 (2020), arXiv:2001.05393 [astro-ph.CO].
- [29] L.-F. Wang, S.-J. Jin, J.-F. Zhang, and X. Zhang, *Sci. China Phys. Mech. Astron.* **65**, 210411 (2022), arXiv:2101.11882 [gr-qc].
- [30] J.-Z. Qi, S.-J. Jin, X.-L. Fan, J.-F. Zhang, and X. Zhang, *JCAP* **12**, 042 (2021), arXiv:2102.01292 [astro-ph.CO].
- [31] S.-J. Jin, L.-F. Wang, P.-J. Wu, J.-F. Zhang, and X. Zhang, *Phys. Rev. D* **104**, 103507 (2021), arXiv:2106.01859 [astro-ph.CO].
- [32] L.-G. Zhu, L.-H. Xie, Y.-M. Hu, S. Liu, E.-K. Li, N. R. Napolitano, B.-T. Tang, J.-d. Zhang, and J. Mei, *Sci. China Phys. Mech. Astron.* **65**, 259811 (2022), arXiv:2110.05224 [astro-ph.CO].
- [33] J. M. S. de Souza, R. Sturani, and J. Alcaniz, *JCAP* **03**, 025 (2022), arXiv:2110.13316 [gr-qc].
- [34] L.-F. Wang, Y. Shao, J.-F. Zhang, and X. Zhang, (2022), arXiv:2201.00607 [astro-ph.CO].
- [35] P.-J. Wu, Y. Shao, S.-J. Jin, and X. Zhang, *JCAP* **06**, 052 (2023), arXiv:2202.09726 [astro-ph.CO].
- [36] S.-J. Jin, T.-N. Li, J.-F. Zhang, and X. Zhang, *JCAP* **08**, 070 (2023), arXiv:2202.11882 [gr-qc].
- [37] S.-J. Jin, R.-Q. Zhu, L.-F. Wang, H.-L. Li, J.-F. Zhang, and X. Zhang, *Commun. Theor. Phys.* **74**, 105404 (2022), arXiv:2204.04689 [astro-ph.CO].
- [38] W.-T. Hou, J.-Z. Qi, T. Han, J.-F. Zhang, S. Cao, and X. Zhang, *JCAP* **05**, 017 (2023), arXiv:2211.10087 [astro-ph.CO].
- [39] J.-Y. Song, L.-F. Wang, Y. Li, Z.-W. Zhao, J.-F. Zhang, W. Zhao, and X. Zhang, *Sci. China Phys. Mech. Astron.* **67**, 230411 (2024), arXiv:2212.00531 [astro-ph.CO].
- [40] S.-J. Jin, S.-S. Xing, Y. Shao, J.-F. Zhang, and X. Zhang, *Chin. Phys. C* **47**, 065104 (2023), arXiv:2301.06722 [astro-ph.CO].
- [41] S.-J. Jin, Y.-Z. Zhang, J.-Y. Song, J.-F. Zhang, and X. Zhang, *Sci. China Phys. Mech. Astron.* **67**, 220412 (2024), arXiv:2305.19714 [astro-ph.CO].
- [42] S.-J. Jin, R.-Q. Zhu, J.-Y. Song, T. Han, J.-F. Zhang, and X. Zhang, (2023), arXiv:2309.11900 [astro-ph.CO].
- [43] T. Han, S.-J. Jin, J.-F. Zhang, and X. Zhang, *Eur. Phys. J. C* **84**, 663 (2024), arXiv:2309.14965 [astro-ph.CO].
- [44] T.-N. Li, S.-J. Jin, H.-L. Li, J.-F. Zhang, and X. Zhang, *Astrophys. J.* **963**, 52 (2024), arXiv:2310.15879 [astro-ph.CO].
- [45] Y.-Y. Dong, J.-Y. Song, S.-J. Jin, J.-F. Zhang, and X. Zhang, (2024), arXiv:2404.18188 [astro-ph.CO].
- [46] L. Feng, T. Han, J.-F. Zhang, and X. Zhang, *Chin. Phys. C* **48**, 095104 (2024), arXiv:2404.19530 [astro-ph.CO].
- [47] L. Bian *et al.*, *Sci. China Phys. Mech. Astron.* **64**, 120401 (2021), arXiv:2106.10235 [gr-qc].
- [48] A. Aguilar *et al.* (LSND), *Phys. Rev. D* **64**, 112007 (2001), arXiv:hep-ex/0104049.
- [49] C. Giunti and M. Laveder, *Phys. Rev. C* **83**, 065504 (2011), arXiv:1006.3244 [hep-ph].
- [50] M. Akbar, H. Quevedo, K. Saifullah, A. Sanchez, and S. Taj, *Phys. Rev. D* **83**, 084031 (2011), arXiv:1101.2722 [gr-qc].
- [51] J. M. Conrad, C. M. Ignarra, G. Karagiorgi, M. H. Shaevitz, and J. Spitz, *Adv. High Energy Phys.* **2013**, 163897 (2013), arXiv:1207.4765 [hep-ex].
- [52] A. A. Aguilar-Arevalo *et al.* (MiniBooNE) (2012) arXiv:1207.4809 [hep-ex].
- [53] C. Giunti, M. Laveder, Y. F. Li, Q. Y. Liu, and H. W. Long, *Phys. Rev. D* **86**, 113014 (2012), arXiv:1210.5715 [hep-ph].
- [54] C. Giunti, M. Laveder, Y. F. Li, and H. W. Long, *Phys. Rev. D* **87**, 013004 (2013), arXiv:1212.3805 [hep-ph].
- [55] J. Kopp, P. A. N. Machado, M. Maltoni, and T. Schwetz, *JHEP* **05**, 050 (2013), arXiv:1303.3011 [hep-ph].
- [56] C. Giunti, M. Laveder, Y. F. Li, and H. W. Long, *Phys. Rev. D* **88**, 073008 (2013), arXiv:1308.5288 [hep-ph].
- [57] S. Gariazzo, C. Giunti, and M. Laveder, *JHEP* **11**, 211 (2013), arXiv:1309.3192 [hep-ph].
- [58] K. N. Abazajian *et al.*, (2012), arXiv:1204.5379 [hep-ph].
- [59] S. Hannestad, I. Tamborra, and T. Tram, *JCAP* **07**, 025 (2012), arXiv:1204.5861 [astro-ph.CO].
- [60] J. M. Conrad, W. C. Louis, and M. H. Shaevitz, *Ann. Rev. Nucl. Part. Sci.* **63**, 45 (2013), arXiv:1306.6494 [hep-ex].
- [61] W. Hu, D. J. Eisenstein, and M. Tegmark, *Phys. Rev. Lett.* **80**, 5255 (1998), arXiv:astro-ph/9712057.
- [62] B. A. Reid, L. Verde, R. Jimenez, and O. Mena, *JCAP* **01**, 003 (2010), arXiv:0910.0008 [astro-ph.CO].
- [63] H. Li and X. Zhang, *Phys. Lett. B* **713**, 160 (2012), arXiv:1202.4071 [astro-ph.CO].
- [64] X. Wang, X.-L. Meng, T.-J. Zhang, H. Shan, Y. Gong, C. Tao, X. Chen, and Y. F. Huang, *JCAP* **11**, 018 (2012), arXiv:1210.2136 [astro-ph.CO].
- [65] J. Hamann, S. Hannestad, and Y. Y. Y. Wong, *JCAP* **11**, 052 (2012), arXiv:1209.1043 [astro-ph.CO].
- [66] Y.-H. Li, S. Wang, X.-D. Li, and X. Zhang, *JCAP* **02**, 033 (2013), arXiv:1207.6679 [astro-ph.CO].
- [67] S. Riemer-Sørensen, D. Parkinson, and T. M. Davis, *Phys. Rev. D* **89**, 103505 (2014), arXiv:1306.4153 [astro-ph.CO].
- [68] E. Giusarma, R. de Putter, S. Ho, and O. Mena, *Phys. Rev. D* **88**, 063515 (2013), arXiv:1306.5544 [astro-ph.CO].
- [69] R. N. Cahn, D. A. Dwyer, S. J. Freedman, W. C. Haxton, R. W. Kadel, Y. G. Kolomensky, K. B. Luk, P. McDonald, G. D. Orebi Gann, and A. W. P. Poon, in *Snowmass 2013: Snowmass on the Mississippi* (2013) arXiv:1307.5487 [hep-ex].
- [70] J. Lesgourgues and S. Pastor, *New J. Phys.* **16**, 065002 (2014), arXiv:1404.1740 [hep-ph].
- [71] J.-F. Zhang, Y.-H. Li, and X. Zhang, *Eur. Phys. J. C* **74**, 2954 (2014), arXiv:1404.3598 [astro-ph.CO].

- [72] X.-Y. Zhou and J.-H. He, *Commun. Theor. Phys.* **62**, 102 (2014), arXiv:1406.6822 [astro-ph.CO].
- [73] M. Costanzi, B. Sartoris, M. Viel, and S. Borgani, *JCAP* **10**, 081 (2014), arXiv:1407.8338 [astro-ph.CO].
- [74] N. Palanque-Delabrouille *et al.*, *JCAP* **02**, 045 (2015), arXiv:1410.7244 [astro-ph.CO].
- [75] J.-F. Zhang, M.-M. Zhao, Y.-H. Li, and X. Zhang, *JCAP* **04**, 038 (2015), arXiv:1502.04028 [astro-ph.CO].
- [76] X. Qian and P. Vogel, *Prog. Part. Nucl. Phys.* **83**, 1 (2015), arXiv:1505.01891 [hep-ex].
- [77] R. B. Patterson, *Ann. Rev. Nucl. Part. Sci.* **65**, 177 (2015), arXiv:1506.07917 [hep-ex].
- [78] R. Allison, P. Caucal, E. Calabrese, J. Dunkley, and T. Louis, *Phys. Rev. D* **92**, 123535 (2015), arXiv:1509.07471 [astro-ph.CO].
- [79] C.-Q. Geng, C.-C. Lee, R. Myrzakulov, M. Sami, and E. N. Saridakis, *JCAP* **01**, 049 (2016), arXiv:1504.08141 [astro-ph.CO].
- [80] Y. Chen and L. Xu, *Phys. Lett. B* **752**, 66 (2016), arXiv:1507.02008 [astro-ph.CO].
- [81] X. Zhang, *Phys. Rev. D* **93**, 083011 (2016), arXiv:1511.02651 [astro-ph.CO].
- [82] Q.-G. Huang, K. Wang, and S. Wang, *Eur. Phys. J. C* **76**, 489 (2016), arXiv:1512.05899 [astro-ph.CO].
- [83] Y. Chen, B. Ratra, M. Biesiada, S. Li, and Z.-H. Zhu, *Astrophys. J.* **829**, 61 (2016), arXiv:1603.07115 [astro-ph.CO].
- [84] M. Moresco, R. Jimenez, L. Verde, A. Cimatti, L. Pozzetti, C. Maraston, and D. Thomas, *JCAP* **12**, 039 (2016), arXiv:1604.00183 [astro-ph.CO].
- [85] J. Lu, M. Liu, Y. Wu, Y. Wang, and W. Yang, *Eur. Phys. J. C* **76**, 679 (2016), arXiv:1606.02987 [astro-ph.CO].
- [86] R. Hada and T. Futamase, *Astrophys. J.* **828**, 112 (2016), arXiv:1606.09091 [astro-ph.CO].
- [87] S. Wang, Y.-F. Wang, D.-M. Xia, and X. Zhang, *Phys. Rev. D* **94**, 083519 (2016), arXiv:1608.00672 [astro-ph.CO].
- [88] S. Kumar and R. C. Nunes, *Phys. Rev. D* **94**, 123511 (2016), arXiv:1608.02454 [astro-ph.CO].
- [89] M.-M. Zhao, Y.-H. Li, J.-F. Zhang, and X. Zhang, *Mon. Not. Roy. Astron. Soc.* **469**, 1713 (2017), arXiv:1608.01219 [astro-ph.CO].
- [90] H. Böhringer and G. Chon, *Mod. Phys. Lett. A* **31**, 1640008 (2016), arXiv:1610.02855 [astro-ph.CO].
- [91] L. Xu and Q.-G. Huang, *Sci. China Phys. Mech. Astron.* **61**, 039521 (2018), arXiv:1611.05178 [astro-ph.CO].
- [92] S. Vagnozzi, E. Giusarma, O. Mena, K. Freese, M. Gerbino, S. Ho, and M. Lattanzi, *Phys. Rev. D* **96**, 123503 (2017), arXiv:1701.08172 [astro-ph.CO].
- [93] R.-Y. Guo, Y.-H. Li, J.-F. Zhang, and X. Zhang, *JCAP* **05**, 040 (2017), arXiv:1702.04189 [astro-ph.CO].
- [94] X. Zhang, *Sci. China Phys. Mech. Astron.* **60**, 060431 (2017), arXiv:1703.00651 [astro-ph.CO].
- [95] L. Chen, Q.-G. Huang, and K. Wang, *Eur. Phys. J. C* **77**, 762 (2017), arXiv:1707.02742 [astro-ph.CO].
- [96] W. Yang, R. C. Nunes, S. Pan, and D. F. Mota, *Phys. Rev. D* **95**, 103522 (2017), arXiv:1703.02556 [astro-ph.CO].
- [97] S. M. Kocsbang and S. Hannestad, *JCAP* **09**, 014 (2017), arXiv:1707.02579 [astro-ph.CO].
- [98] E.-K. Li, H. Zhang, M. Du, Z.-H. Zhou, and L. Xu, *JCAP* **08**, 042 (2018), arXiv:1703.01554 [astro-ph.CO].
- [99] S. Wang, Y.-F. Wang, and D.-M. Xia, *Chin. Phys. C* **42**, 065103 (2018), arXiv:1707.00588 [astro-ph.CO].
- [100] M.-M. Zhao, J.-F. Zhang, and X. Zhang, *Phys. Lett. B* **779**, 473 (2018), arXiv:1710.02391 [astro-ph.CO].
- [101] A. Boyle and E. Komatsu, *JCAP* **03**, 035 (2018), arXiv:1712.01857 [astro-ph.CO].
- [102] S. Vagnozzi, S. Dhawan, M. Gerbino, K. Freese, A. Goobar, and O. Mena, *Phys. Rev. D* **98**, 083501 (2018), arXiv:1801.08553 [astro-ph.CO].
- [103] R.-Y. Guo, J.-F. Zhang, and X. Zhang, *Chin. Phys. C* **42**, 095103 (2018), arXiv:1803.06910 [astro-ph.CO].
- [104] S. Roy Choudhury and S. Choubey, *JCAP* **09**, 017 (2018), arXiv:1806.10832 [astro-ph.CO].
- [105] L. Feng, H.-L. Li, J.-F. Zhang, and X. Zhang, *Sci. China Phys. Mech. Astron.* **63**, 220401 (2020), arXiv:1903.08848 [astro-ph.CO].
- [106] J.-F. Zhang, B. Wang, and X. Zhang, *Sci. China Phys. Mech. Astron.* **63**, 280411 (2020), arXiv:1907.00179 [astro-ph.CO].
- [107] H.-L. Li, J.-F. Zhang, and X. Zhang, *Commun. Theor. Phys.* **72**, 125401 (2020), arXiv:2005.12041 [astro-ph.CO].
- [108] M. Zhang, J.-F. Zhang, and X. Zhang, *Commun. Theor. Phys.* **72**, 125402 (2020), arXiv:2005.04647 [astro-ph.CO].
- [109] P. C. de Holanda and A. Y. Smirnov, *Phys. Rev. D* **83**, 113011 (2011), arXiv:1012.5627 [hep-ph].
- [110] A. Palazzo, *Mod. Phys. Lett. A* **28**, 1330004 (2013), arXiv:1302.1102 [hep-ph].
- [111] J. Hamann and J. Hasenkamp, *JCAP* **10**, 044 (2013), arXiv:1308.3255 [astro-ph.CO].
- [112] M. Wyman, D. H. Rudd, R. A. Vanderveld, and W. Hu, *Phys. Rev. Lett.* **112**, 051302 (2014), arXiv:1307.7715 [astro-ph.CO].
- [113] R. A. Battye and A. Moss, *Phys. Rev. Lett.* **112**, 051303 (2014), arXiv:1308.5870 [astro-ph.CO].
- [114] C. Dvorkin, M. Wyman, D. H. Rudd, and W. Hu, *Phys. Rev. D* **90**, 083503 (2014), arXiv:1403.8049 [astro-ph.CO].
- [115] M. Archidiacono, N. Fornengo, S. Gariazzo, C. Giunti, S. Hannestad, and M. Laveder, *JCAP* **06**, 031 (2014), arXiv:1404.1794 [astro-ph.CO].
- [116] P. Ko and Y. Tang, *Phys. Lett. B* **739**, 62 (2014), arXiv:1404.0236 [hep-ph].
- [117] Y.-H. Li, J.-F. Zhang, and X. Zhang, *Sci. China Phys. Mech. Astron.* **57**, 1455 (2014), arXiv:1405.0570 [astro-ph.CO].
- [118] J.-F. Zhang, Y.-H. Li, and X. Zhang, *Phys. Lett. B* **740**, 359 (2015), arXiv:1403.7028 [astro-ph.CO].
- [119] M. Archidiacono, S. Hannestad, R. S. Hansen, and T. Tram, *Phys. Rev. D* **91**, 065021 (2015), arXiv:1404.5915 [astro-ph.CO].
- [120] J. Bergström, M. C. Gonzalez-Garcia, V. Niro, and J. Salvado, *JHEP* **10**, 104 (2014), arXiv:1407.3806 [hep-ph].
- [121] F. P. An *et al.* (Daya Bay), *Phys. Rev. Lett.* **113**, 141802 (2014), arXiv:1407.7259 [hep-ex].
- [122] J.-F. Zhang, J.-J. Geng, and X. Zhang, *JCAP* **10**, 044 (2014), arXiv:1408.0481 [astro-ph.CO].
- [123] J.-F. Zhang, Y.-H. Li, and X. Zhang, *Phys. Lett. B* **739**, 102 (2014), arXiv:1408.4603 [astro-ph.CO].
- [124] Y.-H. Li, J.-F. Zhang, and X. Zhang, *Phys. Lett. B* **744**, 213 (2015), arXiv:1502.01136 [astro-ph.CO].
- [125] L. Feng, J.-F. Zhang, and X. Zhang, *Eur. Phys. J. C* **77**, 418 (2017), arXiv:1703.04884 [astro-ph.CO].

- [126] M.-M. Zhao, D.-Z. He, J.-F. Zhang, and X. Zhang, *Phys. Rev. D* **96**, 043520 (2017), [arXiv:1703.08456 \[astro-ph.CO\]](#).
- [127] L. Feng, J.-F. Zhang, and X. Zhang, *Sci. China Phys. Mech. Astron.* **61**, 050411 (2018), [arXiv:1706.06913 \[astro-ph.CO\]](#).
- [128] L. Feng, J.-F. Zhang, and X. Zhang, *Phys. Dark Univ.* **23**, 100261 (2019), [arXiv:1712.03148 \[astro-ph.CO\]](#).
- [129] A. M. Knee, D. Contreras, and D. Scott, *JCAP* **07**, 039 (2019), [arXiv:1812.02102 \[astro-ph.CO\]](#).
- [130] L. Feng, D.-Z. He, H.-L. Li, J.-F. Zhang, and X. Zhang, *Sci. China Phys. Mech. Astron.* **63**, 290404 (2020), [arXiv:1910.03872 \[astro-ph.CO\]](#).
- [131] L. Feng, R.-Y. Guo, J.-F. Zhang, and X. Zhang, *Phys. Lett. B* **827**, 136940 (2022), [arXiv:2109.06111 \[astro-ph.CO\]](#).
- [132] E. Di Valentino, S. Gariazzo, C. Giunti, O. Mena, S. Pan, and W. Yang, *Phys. Rev. D* **105**, 103511 (2022), [arXiv:2110.03990 \[astro-ph.CO\]](#).
- [133] P. A. Chernikov and A. V. Ivanchik, *Astron. Lett.* **48**, 689 (2022), [arXiv:2302.05251 \[astro-ph.CO\]](#).
- [134] S. Pan, O. Seto, T. Takahashi, and Y. Toda, (2023), [arXiv:2312.15435 \[astro-ph.CO\]](#).
- [135] L. Verde, T. Treu, and A. G. Riess, *Nature Astron.* **3**, 891 (2019), [arXiv:1907.10625 \[astro-ph.CO\]](#).
- [136] T. Yang, *JCAP* **05**, 044 (2021), [arXiv:2103.01923 \[astro-ph.CO\]](#).
- [137] E. Belgacem, Y. Dirian, S. Foffa, E. J. Howell, M. Maggiore, and T. Regimbau, *JCAP* **08**, 015 (2019), [arXiv:1907.01487 \[astro-ph.CO\]](#).
- [138] S. Vitale, W. M. Farr, K. Ng, and C. L. Rodriguez, *Astrophys. J. Lett.* **886**, L1 (2019), [arXiv:1808.00901 \[astro-ph.HE\]](#).
- [139] P. Madau and M. Dickinson, *Ann. Rev. Astron. Astrophys.* **52**, 415 (2014), [arXiv:1403.0007 \[astro-ph.CO\]](#).
- [140] A. Eichhorn, T. Koslowski, and A. D. Pereira, *Universe* **5**, 53 (2019), [arXiv:1811.12909 \[gr-qc\]](#).
- [141] R. Abbott *et al.* (KAGRA, VIRGO, LIGO Scientific), *Phys. Rev. X* **13**, 011048 (2023), [arXiv:2111.03634 \[astro-ph.HE\]](#).
- [142] X. Zhang, T. Liu, and W. Zhao, *Phys. Rev. D* **95**, 104027 (2017), [arXiv:1702.08752 \[gr-qc\]](#).
- [143] W. Zhao and L. Wen, *Phys. Rev. D* **97**, 064031 (2018), [arXiv:1710.05325 \[astro-ph.CO\]](#).
- [144] L. Wen and Y. Chen, *Phys. Rev. D* **81**, 082001 (2010), [arXiv:1003.2504 \[astro-ph.CO\]](#).
- [145] C. Cutler *et al.*, *Phys. Rev. Lett.* **70**, 2984 (1993), [arXiv:astro-ph/9208005](#).
- [146] B. S. Sathyaprakash and B. F. Schutz, *Living Rev. Rel.* **12**, 2 (2009), [arXiv:0903.0338 \[gr-qc\]](#).
- [147] E. J. Howell, K. Ackley, A. Rowlinson, and D. Coward, (2018), [10.1093/mnras/stz455](#), [arXiv:1811.09168 \[astro-ph.HE\]](#).
- [148] D. Wanderman and T. Piran, *Mon. Not. Roy. Astron. Soc.* **448**, 3026 (2015), [arXiv:1405.5878 \[astro-ph.HE\]](#).
- [149] G. Stratta, L. Amati, R. Ciolfi, and S. Vinciguerra, *Mem. Soc. Ast. It.* **89**, 205 (2018), [arXiv:1802.01677 \[astro-ph.IM\]](#).
- [150] L. Speri, N. Tamanini, R. R. Caldwell, J. R. Gair, and B. Wang, *Phys. Rev. D* **103**, 083526 (2021), [arXiv:2010.09049 \[astro-ph.CO\]](#).
- [151] C. M. Hirata, D. E. Holz, and C. Cutler, *Phys. Rev. D* **81**, 124046 (2010), [arXiv:1004.3988 \[astro-ph.CO\]](#).
- [152] B. Kocsis, Z. Frei, Z. Haiman, and K. Menou, *Astrophys. J.* **637**, 27 (2006), [arXiv:astro-ph/0505394](#).
- [153] N. Aghanim *et al.* (Planck), *Astron. Astrophys.* **641**, A6 (2020), [Erratum: *Astron. Astrophys.* 652, C4 (2021)], [arXiv:1807.06209 \[astro-ph.CO\]](#).
- [154] F. Beutler, C. Blake, M. Colless, D. H. Jones, L. Staveley-Smith, L. Campbell, Q. Parker, W. Saunders, and F. Watson, *Mon. Not. Roy. Astron. Soc.* **416**, 3017 (2011), [arXiv:1106.3366 \[astro-ph.CO\]](#).
- [155] A. J. Ross, L. Samushia, C. Howlett, W. J. Percival, A. Burden, and M. Manera, *Mon. Not. Roy. Astron. Soc.* **449**, 835 (2015), [arXiv:1409.3242 \[astro-ph.CO\]](#).
- [156] S. Alam *et al.* (BOSS), *Mon. Not. Roy. Astron. Soc.* **470**, 2617 (2017), [arXiv:1607.03155 \[astro-ph.CO\]](#).
- [157] D. M. Scolnic *et al.* (Pan-STARRS1), *Astrophys. J.* **859**, 101 (2018), [arXiv:1710.00845 \[astro-ph.CO\]](#).
- [158] A. Lewis and S. Bridle, *Phys. Rev. D* **66**, 103511 (2002), [arXiv:astro-ph/0205436](#).
- [159] <https://www.et-gw.eu/index.php/etsensitivities/>.
- [160] <https://cosmicexplorer.org/sensitivity.html>.
- [161] J.-P. Zhu *et al.*, *Astrophys. J.* **942**, 88 (2023), [arXiv:2110.10469 \[astro-ph.HE\]](#).